Part II: Frequency Offset Acquisition and Tracking Algorithms

Mohamed K. Nezami
Mnemonics Inc.
3900 Dow Rd
Melbourne, FL 32934

In part I, several algorithms were developed for carrier frequency offset acquisition. The algorithms estimate the offset frequency independent of the carrier phase errors or symbol timing. Phase errors are estimated and corrected, after frequency estimation and correction as shown in figure 1 of part 1. In part II, phase estimation algorithms using open loops and closed loops techniques are presented, a particular application example will be the use of both techniques for acquiring and tracking short TDMA burst satellite signals. Finally, practical methods for implementing these algorithms using commercial DSP chips are introduced.

IV.5: Open Loop Mth Power Carrier Phase Tracking Algorithm

As has been indicated earlier, carrier tracking takes place after frequency offsets have been removed, carrier phase tracking is implemented as shown in figure 1 of part I, where the phase error is estimated by calculating the average rotation of the constellation points. Its is assumed that we are sampling once per symbol at the instants of maximum aye opening. For small residual frequency offset Δf_r resulting from an imperfect frequency offset algorithm performance, the phase variation over one burst is $\theta = 2\pi\Delta f_r LT$, if the observation interval for phase estimation is kept relatively short, this phase variation can be assumed negligible. The carrier phase is estimated by the use of a non-linearity applied to the matched filter complex samples given by (17)

$$s(kT) = F\left(|z(kT)|\right)e^{jM\arg(z(kT))} \quad (17)$$

where $F\left(|z(kT)|\right) = \left(|z(kT)|\right)^{\ell}$ is the non-linearity performed on the magnitude of the samples out of the frequency acquisition and correction algorithm. The value of non-linearity order (ℓ) was investigated by Viterbi. For MPSK modulations, the value of the non-linearity order ℓ can be 4, 8 or 16. Our simulations have shown that $\ell = M$ and equal to 4 was best suited for moderate signal to noise ratios [part I, 6]. Operating on equation 17, the M^{th}-power phase estimates is given by (18)

$$\hat{\theta} = \frac{1}{M}\tan^{-1}\left\{\frac{\sum_{k=0}^{L}\mathrm{Im}[s(kT)]}{\sum_{k=0}^{L}\mathrm{Re}[s(kT)]}\right\} \quad (18)$$

here the range of estimation for this algorithm is limited to $-\frac{\pi}{2M} \le \theta \le \frac{\pi}{2M}$. To make this estimate more robust against fading [3], specially during the presence of fading or residual frequency offsets, the phase estimates (18) are post processed using a low order smoothing filter that will reduce their variance. The post processing filter and the M-

power phase estimation algorithm implementation is shown in Figure 7. This post-processing filter can be thought of being a first order Kalman filter smoother [3]. As a result of post processing, the phase is given by (17)

$$\tilde{\theta}_k = \mu\hat{\theta}_k + (1-\mu)\hat{\theta}_{k-1} \qquad (17)$$

where $0 \le \mu \le 1$ is the convergence factor. Through simulations, we have found that the value of μ which controls the time constant of the filter, actually can be optimized to yield better performance based on the statistics of fade or the maximum residual frequency offset present [3]. Figure 8 shows the algorithm performance using QPSK signal in AWGN with an intentional phase error. The figure shows an estimation range of $-22.5^0 \le \theta \le 22.5^0$.

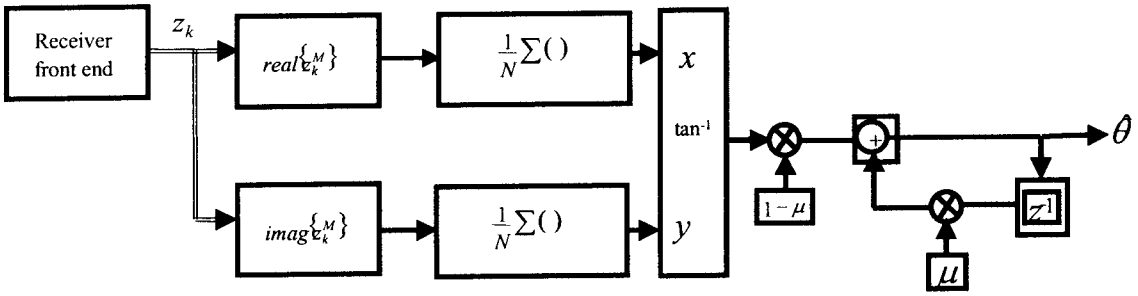

Figure 7: Open Loop M[th] power carrier phase estimator

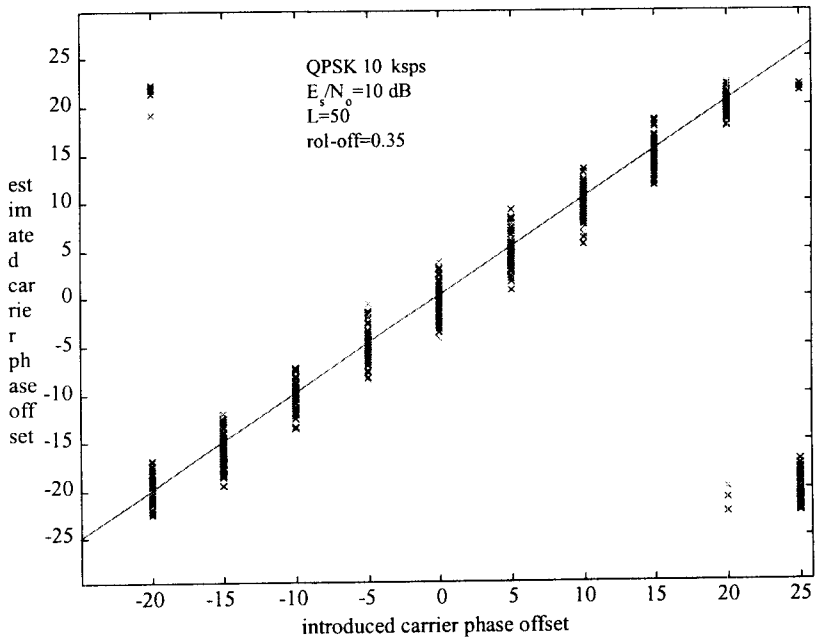

Figure 8: Phase recovery process of M[th] power carrier phase algorithm

V. Digital Implementation of Satellite Carrier Acquisition and Tracking

Most satellite systems utilize TDMA, where multiple users share the same channel by using the bandwidth for discrete intervals of time slots. Only one user can access the channel at any instant in time. Time slots are assigned by a netwolrk controller for each frame (user). Each terminal has unique phase and frequency offset resulting in unpredictable carrier changes from message to message. To aid acquisition, each message or frame has a preamble or training sequence, which is transmitted as the initial part of each communications burst. The preamble format usually is continuous wave (CW) carrier followed by a dot pattern (alternating or repeating sequence of l's and O's). The CW sequence (all O's) creates a tone that is commonly used by receivers to recover frequency offsets and tracking using some form of feedback loops, such as Costas acquisition and tracking loop. The alternating sequence following the CW part in the burst creates a sine wave at the receiver that has a frequency at half the symbol rate, which is used for symbol synchronization.

Frequency offsets in MobileSat communication terminals are experienced due to several factors, oscillator frequency-uncertainty, oscillators drift, and Doppler effects arising from vehicular motion with respect to the satellite. Depending on the carrier frequency and satellite and ground receiver's relative velocity, such frequency offsets can vary from few hundred Hertz up to several kilohertz. LEO and ICO satellites are located at heights of 10,000 - 20,000 kms above the equator, and have a relative velocity of 1500 m/s operating at 2 GHz, this results in Doppler shifts as high as 10 kHz. GE0 satellites are located at height of 36,000 km and operate at frequency of 1.5 GHz; or C/KU-band, while the satellite is fixed relative to earth, the relative mobile speed of 100 km/hr creates a Doppler shift of up to 138 Hz for L-band signals. For aircraft with speeds up to 1000 km/hr, the maximum Doppler can be as high as 1800 Hz.

There are several methods employed to estimate such Doppler and carrier drifts, then correct for them. First method is by tuning the reference NC0 to an initial known offset, during the first portion of the TDMA, the loop is configured to irnplement a frequency locked loop by using wide loop bandwidth to be able to pull in large frequency offsets, and frequency acquisition occur within few inverse loop bandwidth values with high probability. After the loop having locked, the loop bandwidth is narrowed to implement a phase lock loop to track out phase errors. A second approach is to use a fixed loop bandwidth, however sweep the frequency oscillator (NCO) of the receiver over the uncertainty region (+ Af_{max}) at sufficiently low rate so as to enable the narrow loop to lock. A third approach has recently been utilized due to the introduction of high speed, low cost DSPs, is to use DFT aided acquisition [6]. The DFT operation would determine the initial frequency offset in relatively short processing time while the loop is open, then the **NC0** is programmed to the conjugate of that offset resulting in reducing the total frequency offset to a residual offset which is within the pull-in range of the Costas loop.

V.1 Carrier Acquisition and Tracking using Feedback Loops

There are several ways such loops are implemented. The frequency error can be generated in several methods, one such method is to use the M-power offset estimation algorithm in conjunction with a NCO and a complex multiplier, another method is to use the dot and cross product terms of the differential detector (equation 7, part I). Figure 9 shows such implementation. Here the loop is a closed-loop servo mechanism that uses negative feedback to keep the frequency offset of the NCO equal to the complex conjugate of the incoming offset-baseband carrier frequency. The carrier error loop filter is designed with parameters K_{lead} and K_{lag} such that they minimize phase and offset errors, meanwhile yield minimum acquisition time and a narrow loop bandwidth. Both parameters can be adaptive to change the loop bandwidth, so it is wide during signal acquisition, but narrow during tracking. The frequency error detector used, accommodates both QPSK and BPSK modulations. The M[th]-power nonlinearity is sued for phase and frequency tracking when the signal is modulated. If there are no modulations (CW), such as the case at the beginning of most TDMA bursts, the non-linearity can be removed for maximum noise performance.

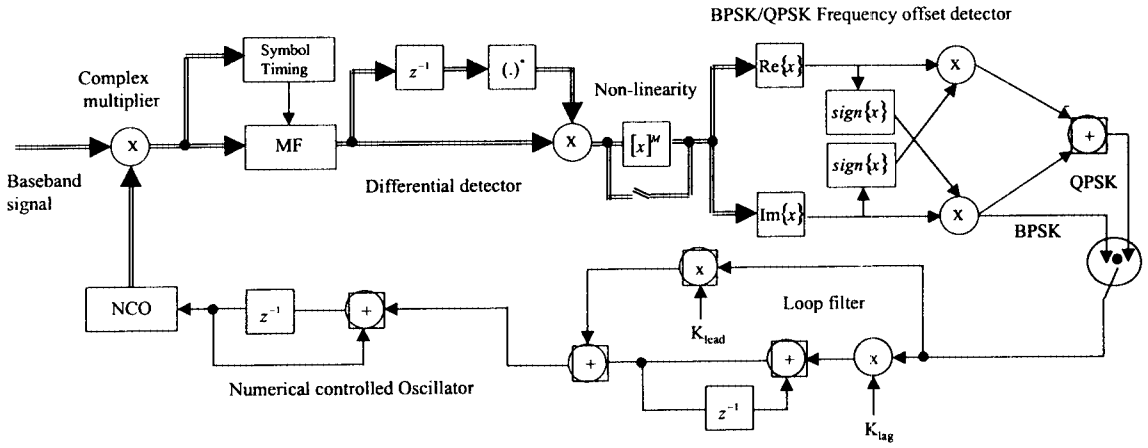

Figure 9: QPSK/BPSK Feedback carrier offset acquisition and tracking loop.

The loop coefficients design starts by using equation 1 in part I, with a given desired t_{acq} and ς, phase detector gain of $K_{phi} = \frac{2^{12}}{\pi}$, and 32 bit NCO again of $K_{NCO} = \frac{2\pi F_{clk}}{2^{32}}$.

The loop parameters are given by (20) and (21)

$$K_{lag} = \frac{4\pi f_n \varsigma}{K_{phi} K_{NCO}} \qquad (20)$$

$$K_{lead} = \frac{4\pi^2 f_n^2}{K_{phi} K_{NCO}} \qquad (21)$$

Where f_n is the natural loop frequency.

V.2. DFT-Aided Open Loop Frequency Acquisition and Tracking

To circumvent problems associated with feedback Costas loops. in figure 9, such as instabilities, design and implementation difficulties, speed of convergence, and preamble utilization, is to use a modified feed forward open loops by extending their capture range to frequency offsets that are larger than 10% of the data rate. Therefore making them able to cope with typical mobile satellite carrier offsets that are of the order of several kilo-Herts. A modified feed forward techniques proposed here, that does not suffer from hang-ups, and can acquire signals with relatively short time, while using random symbols and not constrained to using a dedicated CW portion of the preamble. Furthermore has an extended capture range beyond the estimation range of conventional feed forward algorithms that are emploYed previously.

While the digital implementation of conventional Costas loops and feed forward loops are implemented after the matched filter, resulting in limiting the frequency offset acquisition range, as a result, the matched filter attenuates signals with large frequency offsets that lies outside its pass band. The new proposed scheme is implemented prior to the channel-matched filter by using a simple low pass filter that has a pass band equal to 2Af.,, Hz. The algorithm is primarily developed for carrier acquisition and tracking of signals received from UHF-Military satellites operating with bursts of variable data rates from 1200 to 19200 symbols/s, and a burst duration of 100 to 400 milliseconds. The satellite signal is acquired first at low resolution using relatively sh.ort DFT, which brings large frequency offsets to such offsets that are within the capture range of feed forward algorithm, then the feed forward loop fine tunes the small offsets by estimating the carrier offset with variances less than lo? Unlike Costas loop, the proposed algorithm does not rely on the use of the CW portion of the burst for initial acquisition and phase tracking, instead it utilizes the alternating sequence which does not have to have synchronized symbols, it only utilizes the spectral contents of the alternating sequence. The initial acquisition is performed based on the simple fact that an alternating sequence pattern yields a line spectra with tones at a frequencies of f = Af + $nR, /2$ Hz, where n is an integer. Figure 10 shows a TDMA QPSK burst with a preamble of alternating sequence running at 40 ksps and 10,000 symbols/s. The figure (bottom) shows the spectral contents of the captured signal, where the presence of two spectral peaks at f = Af k $R,/2$, or 4 and 6 kHz. To demonstrate the proposed algorithm, let's assume a satellite signal that experiences a carrier offset with a range Iof Af , where -5kHz ,< Af <5kHz, with $f,$ = 40 $kHz, R,$ = IO, 000 symbols/s, and a bin size that is equal to the maximum frequency range of the Feed forward algorithm. Figure 11 shows the performance of the algorithm in tracking the offset carrier of Af = +5kHz. The figure shows that by combining DFT and feed forward algorithms in a ca;scade form, a powerful algorithm become apparent which can overcome many of the problems associated with conventional Costas and Feed forward algorithms used for wide band acquisition and tracking.

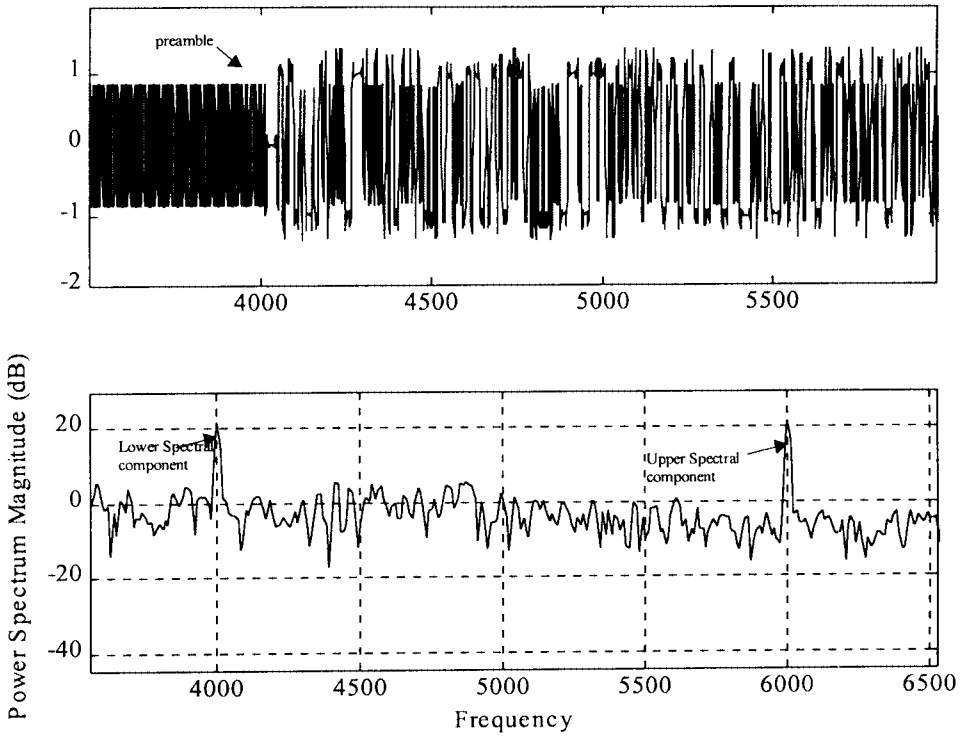

Figure 10: QPSK Satellite TDMA burst.

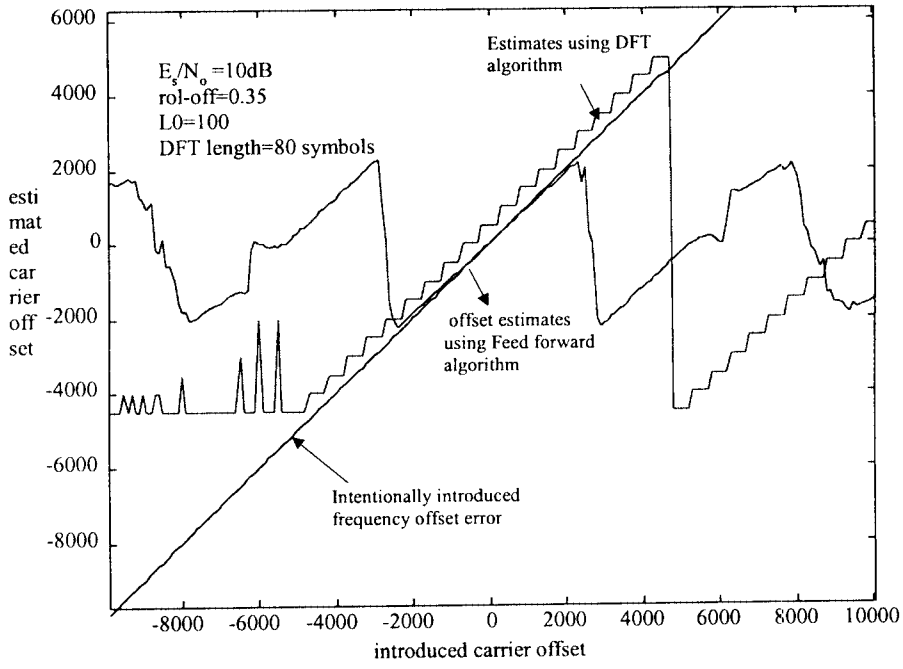

Figure 11: Comparison of feed forward and DFT based frequency offset estimation algorithms

VI. DSP Implementation

Since digital signal processors have no capabilities to do complex mathematical functions, such as $|x|$, $\tan^{-1}(x)$, x/y, and $\sqrt{x}$ functions that are used in the implementation of both frequency offset acquisition and phase tracking algorithm. It is necessary to use approximation to be able to implement such algorithms suing available DSP chips.

1. Magnitude approximation: Magnitude calculation of a complex sample signal is a difficult one since it involves the computation of the square root function which is given by $|I + jQ| = \sqrt{I^2 + Q^2}$. An approximation to this is obtained through use of mathematical expansion given by (22)

$$|I + jQ| = \begin{cases} I + 0.375Q & I > Q \\ Q + 0.375I & else \end{cases} \qquad (22)$$

Figure 12 shows a simulation of this approximation in comparison with the actual function.

2. Division approximation: Division also presents a time consuming and tedious operation for most DSP chips, one way to circumvent this problem is by transforming the division $\frac{x}{y}$ to a multiplication, or $x(1/y)$. An approximation for $1/y$, where $0.5 \le y \le 1$ is given by (23)

$$1/y = 2.5859y^2 - 5.8182y + 4.2424 + \ldots \qquad (23)$$

Using equation (23) the mathematical division becomes (24)

$$\frac{x}{y} = x\{2.5859y^2 - 5.8182y + 4.2424\} \qquad (24)$$

Equation (24) is simpler to implement, since it avoids the use of binary shifting operation that is usually performed when implementing division using DSP chips.

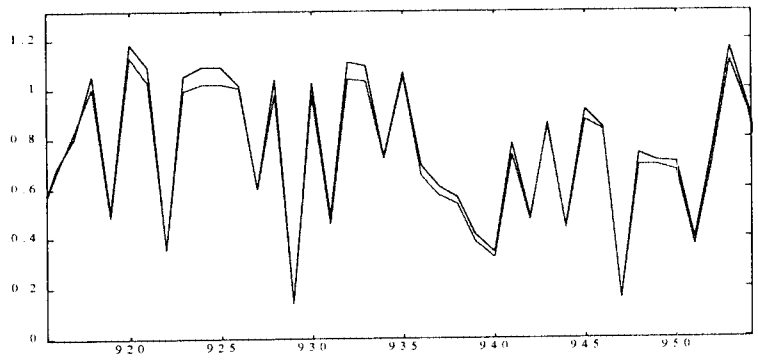

Figure 12: Magnitude approximation algorithm versus actual vector magnitude

3. $\tan^{-1}(x)$ Approximation: $\tan^{-1}(x)$ not only needs table look up to be implemented, but it yields correct answer only in the first two quadrants, or for angles from 0° to 180°. Figure 13 shows an algorithm proposed here that present an approximation to solving the $\tan^{-1}(x)$ function that is implementable using DSP chips. The approximation is given by (25)

$$\arg\{x_k\} = \begin{cases} -\frac{\pi}{4} ratioI(k) + \frac{\pi}{4} & 0^{\circ} \le \theta \le 90^{\circ} \\ -\frac{\pi}{4} ratioII(k) + 3\frac{\pi}{4} & 90^{\circ} \le \theta \le 180^{\circ} \end{cases} \quad (25)$$

Here x can be $\left[z_k z^*_{k-N}\right]^M$ for the frequency estimation algorithm (9), or $[z_k]^M$ for the phase tracking algorithm (18). *ratioI (k)* and *ratioII (k)* are a Lagrange quadratic equations obtained by numerical analysis techniques [1] given by (26)

$$ratioI(k) = \frac{\mathrm{Re}\{z_k z^*{}_{k-N}\} - abs[\mathrm{Im}\{z_k z^*{}_{k-N}\}]}{abs[\mathrm{Im}\{z_k z^*{}_{k-N}\}] + \mathrm{Re}\{z_k z^*{}_{k-N})\}} \quad (26a)$$

and

$$ratioII(k) = \frac{\mathrm{Re}\{z_k z^*{}_{k-N}\} + abs[\mathrm{Im}\{z_k z^*{}_{k-N}\}]}{abs[\mathrm{Im}\{z_k z^*{}_{k-N}\}] - \mathrm{Re}\{z_k z^*{}_{k-N}\}} \quad (26b)$$

The location of the angle with reference to the quadrant I and II can be found through the sign of $\mathrm{Re}\{z_k z^*{}_{k-N}\}$, while the location of the angle in Quadrant III and IV can be found by checking the sign of $\mathrm{Im}\{z(k)z^*(k-N)\}$ as shown in figure 13a.

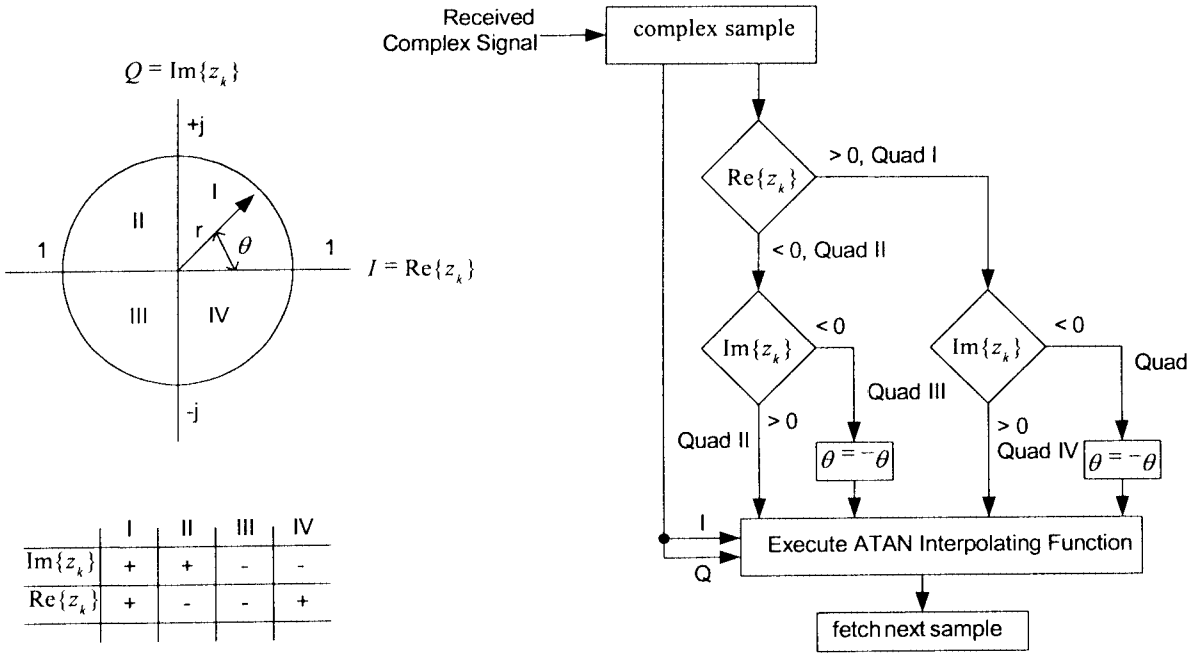

	I	II	III	IV
$\mathrm{Im}\{z_k\}$	+	+	-	-
$\mathrm{Re}\{z_k\}$	+	-	-	+

(13a)

(13b)

Figure 13: *arg{x}* DSP estimation algorithm

The algorithm checks the sample's sign of the real part (i.e., *sign{I}),* for negative *I(k),* the angle must be in quadrant II, otherwise its in Quadrant I. The sign of the imaginary part (i.e., *sign{Q}*) indicates whether the angle is in Quadrant III or Quadrant IV, which then inverts the angle value. This is performed such that the computation is only needed to be performed over quadrant I and II. For angles in quadrant III and IV, only inversion is needed. Figure 14 shows the algorithm performance compared to the actual $\tan^{-1}(x)$. Clearly very small error is noticed especially at the interpolation points of $0^0, \pi/4, \pi/2, 3\pi/4$, and π. If more accuracy is required, a higher order polynomial can be used [1] to compute *ratioI* and *ratioII.* Another attractive feature of this algorithm lies in the fact that amplitude variation in both Q and I, does not effect the angle estimation in (26). This is useful in particular with cases where multi-path fading attenuation is present due to mobile terrain effects.

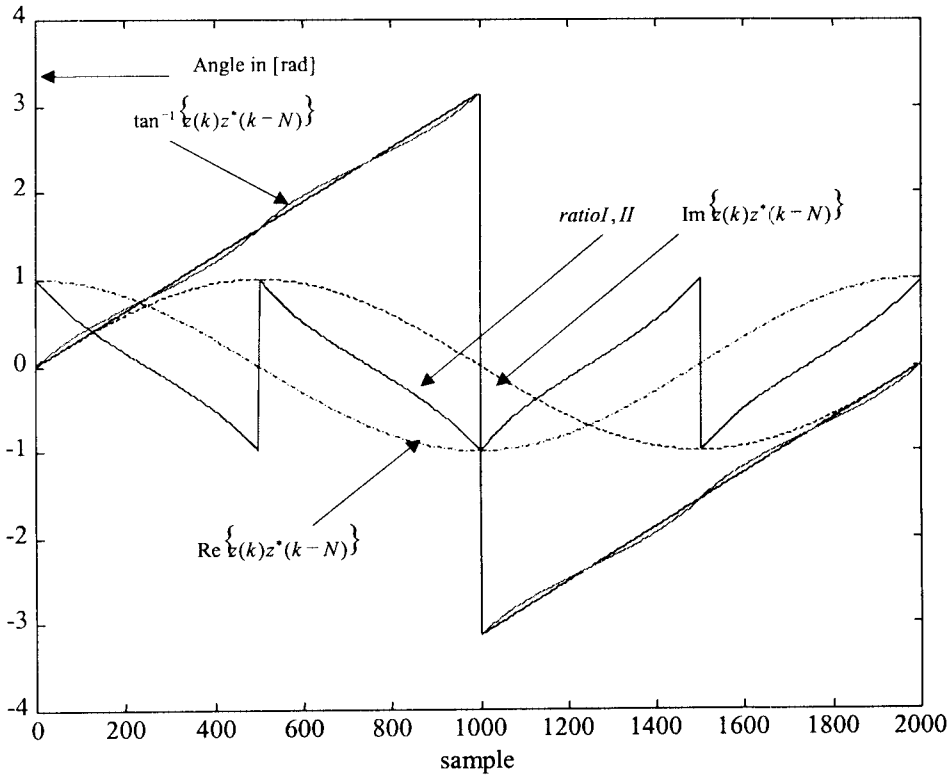

Figure 14: *arg{x}* DSP algorithm performance

The algorithm in (9) in conjunction with (25) was implemented using Texas Instrument C50 processor, with sampling rate of 150 kHz and a matched filter signal of 25 kHz having a frequency offset introduced by the satellite dynamics and of $\Delta f = \pm 20$ kHz. As a result of the frequency offset present, the digital baseband signal had a frequency of 5 kHz to 45 kHz. The algorithm performance was excellent, except that care had to be taken for frequency offsets at the high end of the spectrum, where the oversampling rate was only 3.30, this causes a sample to sample maximum phase variation of $\theta_{\max}(k) = 360^0 f / f_s$, or $\theta = 108^0$ of phase shift, as a result, only 72^0 of phase margin is available, before the sample to sample phase shift introduces ambiguity due to noise spikes while operating at low SNR. Here, often cycle slips will wrap the phase around to the opposite side of the estimation interval, resulting in bad estimates, this was very annoying in the lab, but further post processing and proper filtering resulted in improved receiver performance.

VII. Conclusion

Feedback and feed forward techniques for carrier frequency acquisition and phase tracking algorithms were presented. New algorithms that can acquire signals with large offsets were introduced and characterized. Characterization of these algorithms was conducted using simulations. Practical DSP implementation of these algorithms were introduced and discussed.

Acknowledgment

The author would like to acknowledge Dr. Sudhakar of Florida Atlantic University, Dr. Bard and Mr. H. Weeter of Mnemonics Inc. for contributing to this work.

References

1. Numerical Recipes in C : The Art of Scientific Computing; William H. Press et al; 1999.

2. J. Bard, M. Nezami, and M Diaz "Data Recovery in Differentially Encoded Quadrature Phase Shift keying", Milcom2000, Los Angeles, CA, Oct. 2000.

3. J. M. Nezami and Bard, " Preamble-less carrier recovery in fading channels", Milcom2000, Los Angeles, CA, Oct. 2000.

4. Henry Helmken, Satellite communication class notes, Florida Atlantic University, 1998.

5. Mnemonics Inc., internal designs review of UHF satellite Modem.

6. B. Shah, S. Hinedi, and J. Holmes, "Comparison of four FFT-Based Frequency Acquisition Techniques", NASA tech. brief Vol. 17, No 10, October 1993.

7. Umberto Mengali and M. Moreli, "Data-Aided Frequency Estimation for Burst Digital Transmission", IEEE trans. Communications, Vol. 45, No. 1, January 1997.